Electronic Supplementary Material (ESI) for Journal of Materials Chemistry A.

Revealing the Absence of Carbon in Aprotic Li–CO_2 Batteries: A Mechanism Study Toward CO_2 Reduction Under a Pure CO_2 Environment

Kevin Iputera,[a] Jheng-Yi Huang,[a] Shu-Chih Haw,[b] Jin-Ming Chen,[b] Shu-Fen Hu[c,*] and Ru-Shi Liu[a,*]

[a]Department of Chemistry, National Taiwan University, Taipei 106, Taiwan.

[b]National Synchrotron Radiation Research Center, Hsinchu 30076, Taiwan.

[c]Department of Physics, National Taiwan Normal University, Taipei 116, Taiwan.

* Corresponding authors: Ru-Shi Liu (email: rsliu@ntu.edu.tw); Shu-Fen Hu (email: sfhu.hu@ntnu.edu.tw).

Discussion S1: Calculation of the weight of carbon formed in the discharge process.

The calculation assumes that all the applied current is used to reduce CO_2 to C. Thus, the weight of carbon formed in the discharge process can be described by the following equation:

$$W_C = \frac{Q \times W_{Cathode} \times 3.6\left(\frac{C}{mAh}\right) \times M}{n \times F}$$

W_C is the weight of formed C (g), Q is the discharge capacity (mAh g_c^{-1}), $W_{Cathode}$ is the weight of cathode (g), n is the number of electron transfer in the cell equation (Equation 2) and is equal to 4, and F is the Faraday constant (C mol^{-1}, 96485 C mol^{-1}). M is the molecular weight of carbon which is 12 (Da).

Discussion S2: Calculation of the effect of trace O_2.

The amount of O_2 required for the reaction can be calculated using the following equation:

$$V_{O_2} = \frac{W_{O_2}}{D_{O_2}} = \frac{Q \times W_{Cathode} \times 3.6\left(\frac{C}{mAh}\right)}{n \times F \times D_{O_2}}$$

V_{O_2} is the volume of O_2 (L), W_{O_2} is the weight of O_2 (g), D_{O_2} is the density of O_2 (g L^{-1}, NTP value = 1.331 g L^{-1}), Q is the discharge capacity (mAh g^{-1}), $W_{Cathode}$ is the weight of cathode (g), n is the number of electron transfer in the cell equation (Equation 6) and is equal to 2, and F is the Faraday constant (C mol^{-1}, 96485 C mol^{-1}).

Discussion S3: Derivation of the redox potential of mixed electrochemical/chemical reaction.

If a given reaction

$$\mathrm{A + Y + ne^{-} \rightarrow Z}, \ \Delta G_{tot} = -nFE_{tot}$$

can be divided into n+1 individual elemental steps:

$$\mathrm{A + e^{-} \rightarrow B}, \ \Delta G_1 = -FE_1$$

$$\mathrm{B + e^{-} \rightarrow C}, \ \Delta G_2 = -FE_2$$

$$\vdots$$

$$\mathrm{W + e^{-} \rightarrow X}, \ \Delta G_n = -FE_n$$

$$\mathrm{X + Y \rightarrow Z}, \ \Delta G_c$$

We have the following equation:

$$\Delta G_{tot} = \Delta G_1 + \Delta G_2 + \cdots + \Delta G_n + \Delta G_c$$

$$-nFE_{tot} = -FE_1 - FE_2 - \cdots - FE_n + \Delta G_c$$

$$E_1 + E_2 + \cdots + E_n = \frac{1}{F}\Delta G_c + nE_{tot}$$

Since ΔG_c needs to be negative for a chemical reaction to occur spontaneously, the inequality can be written as

$$E_1 + E_2 + \cdots + E_n < nE_{tot}$$

For the total reaction to happen, the potential needs to be lower than the smallest one among all E_x. Thus, for a mixed electrochemical/chemical reaction, the highest reaction potential can be obtained only when all E_x share the same value and that $\Delta G_c \rightarrow 0$. Note that in the demonstrated reaction, Y represents the species that participate chemically in the reaction. The individual elementary steps can be in any given order, and the derivation can still hold.

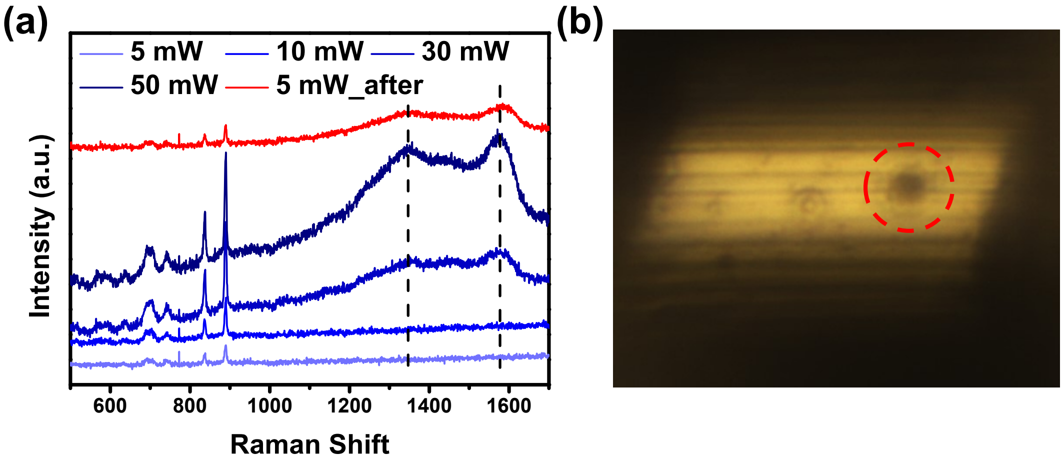

Fig. S1 (a) Raman spectra of a gold cathode measured under different laser power in a Li–CO_2 battery. (b) Optical image of the gold mesh after illumination under 50 mW-laser.

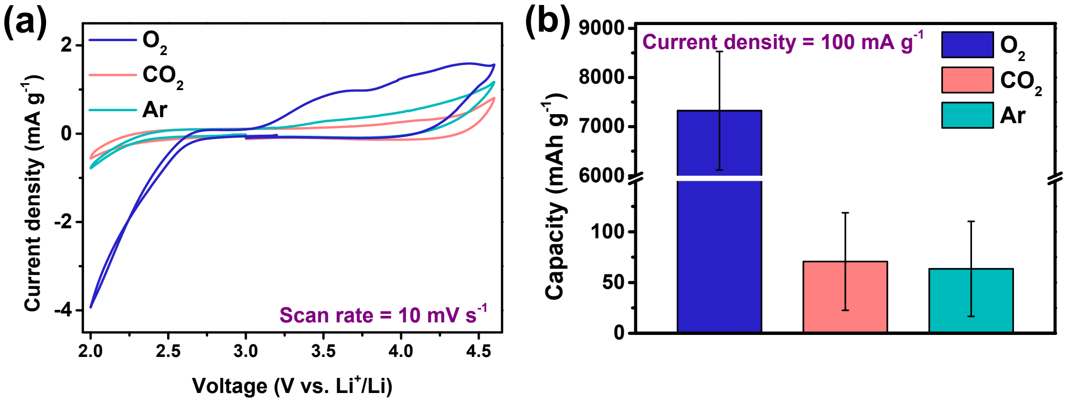

Fig. S2 (a) Cyclic voltammetry (CV) tests and (b) statistics on the full-discharge capacity of Li–gas batteries under three different gas atmospheres. Carbon nanotubes coated on stainless steel mesh (CNTs/SS) were used as working electrodes and cathode, respectively, in both tests.

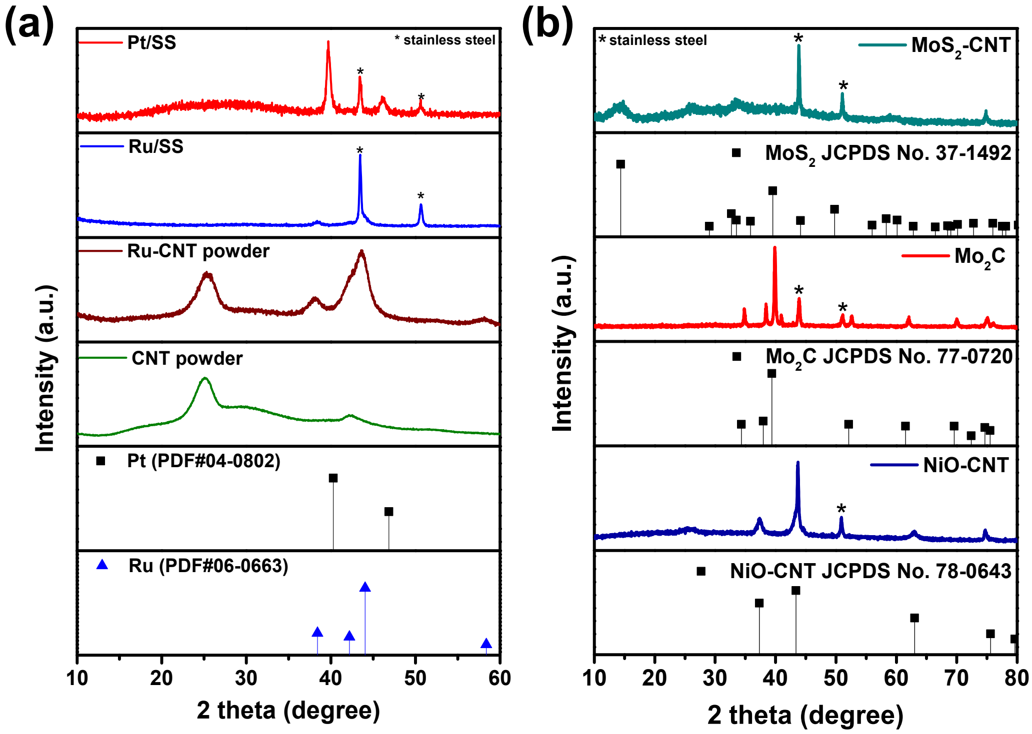

Fig. S3 (a) X-ray diffraction (XRD) patterns of cathode materials. (b) Full-discharge capacities of Li–CO_2 batteries with three different cathodes. The galvanostatic full-discharge tests are all performed with a current density of 100 mA g^{-1} and a cutoff potential of 2 V.

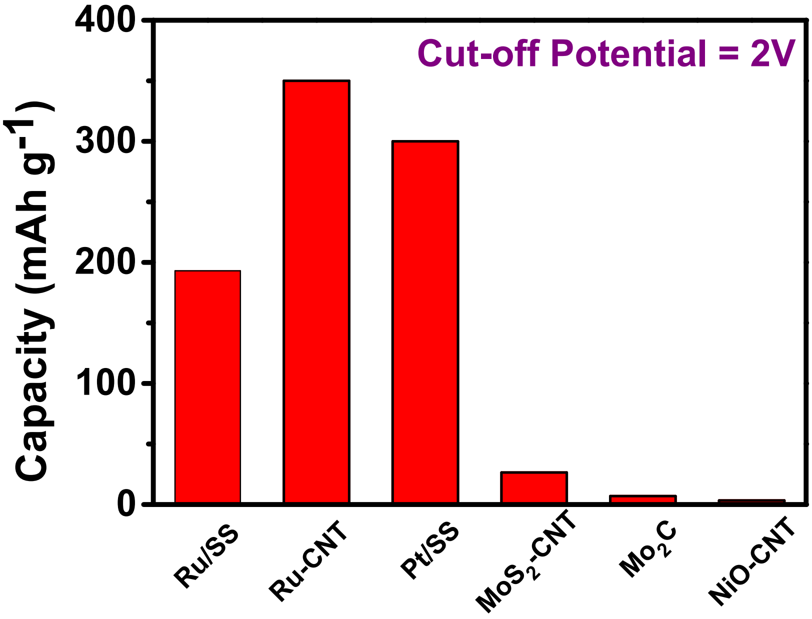

Fig. S4 Full-discharge capacities of Li–CO_2 batteries with five different cathodes. For Pt/SS and Ru/SS, the current density is 15 mA g^{-1} to obtain considerable capacity. The rest of the galvanostatic full-discharge tests are all performed with a current density of 100 mA g^{-1} and a cutoff potential of 2 V.

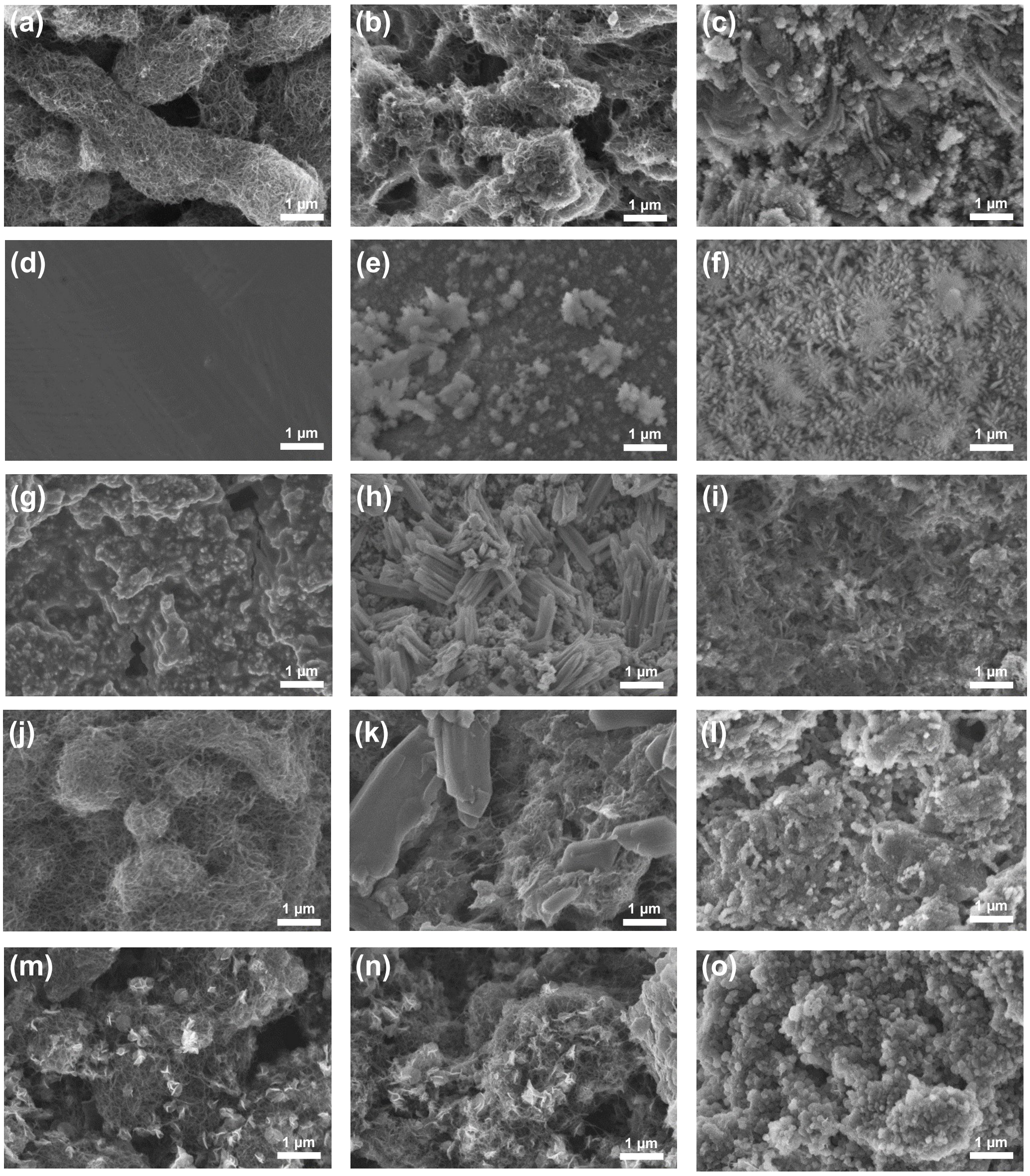

Fig. S5 SEM images of (a) pristine CNTs, (b) 2V-CNTs, (c) 1V-CNTs, (d) pristine Pt, (e) 2V-Pt, (f) 1V-Pt, (g) pristine MoS_2/CNT, (h) 2V-MoS_2/CNT, (i) 1V-MoS_2/CNT, (j) pristine Mo_2C, (k) 2V-Mo_2C, (l) 1V-Mo_2C, (m) pristine NiO/CNT, (n) 2V-NiO/CNT, and (o) 1V-NiO/CNT electrodes.

The SEM images of discharged cathodes show clear evidence of products formation. While the 2V-samples show a relatively small amount of formed species, the 1V-samples are covered with largely formed products. The clear formation of the products upon pristine electrode structures allows further characterization with ease.

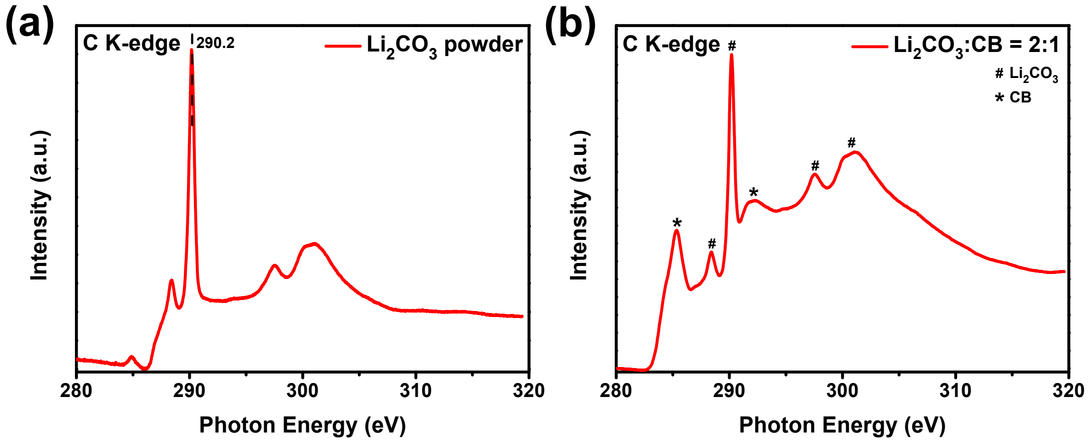

Fig. S6 Soft X-ray absorption spectroscopy (SXAS) profiles of (a) Li_2CO_3 and (b) Li_2CO_3/carbon black mixture with a molar ratio of 2:1.

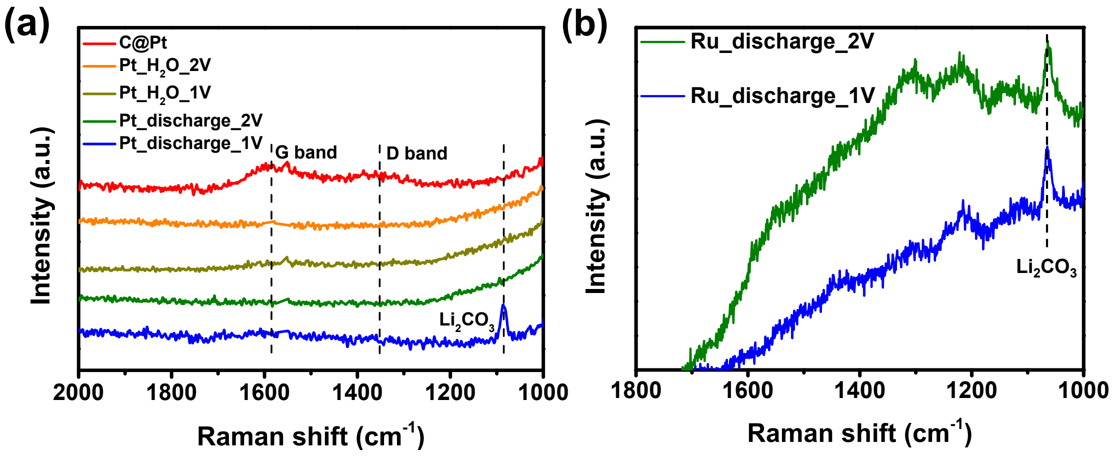

Fig. S7 Raman spectra of (a) Pt/SS with different treatments and (b) Ru/SS after discharge. 532 nm laser was used as the excitation source for all measurements.

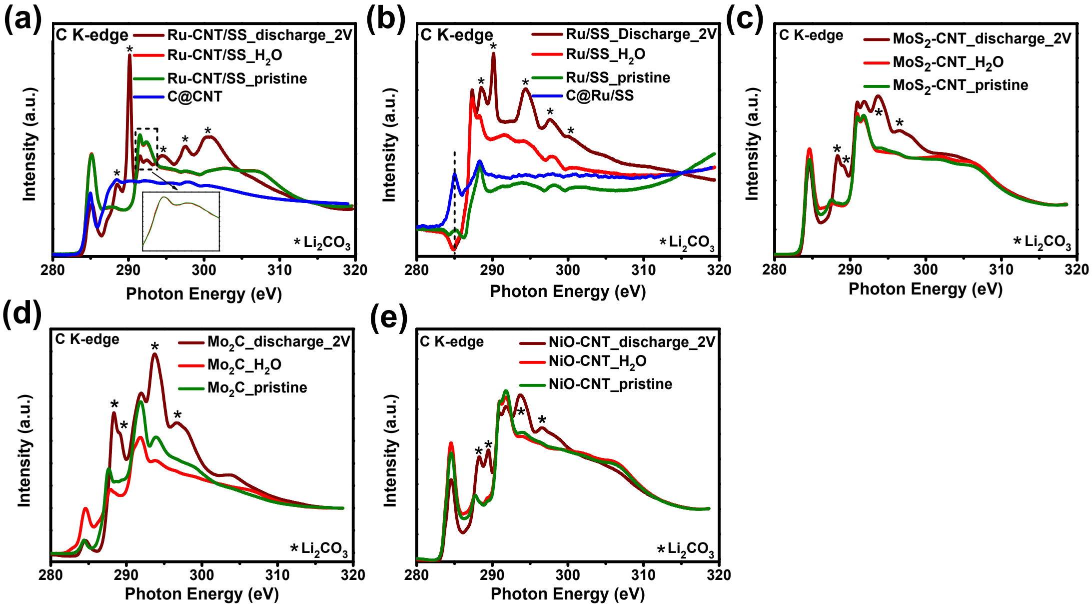

Fig. S8 Soft X-ray absorption spectra (SXAS) of (a) Ru-CNT/SS, (b) Ru/SS, (c) MoS_2-CNT, (d) Mo_2C, and (e) NiO-CNT cathodes under different treatments. The inset of (a) shows the magnification of the framed region.

In Fig. S8a, Ru decorated carbon nanotubes coated on stainless steel mesh (Ru-CNT/SS) are used as cathodes to conduct discharge tests above 2 V. The SXAS results resemble the ones in Fig. 1c. Li_2CO_3 is again formed on the discharged Ru-CNT/SS (brown curve) and can be completely removed after H_2O washing treatment (red curve). When stacking SXAS profiles of H_2O-washed and pristine Ru-CNT/SS, the difference can hardly be found, showing that no carbon is formed after discharge. In Fig. S8b, Ru sputtered stainless steel mesh (Ru/SS) is prepared to reproduce the work done by Yang *et al.*[2] The small peak at around 285 eV in the pristine sample (green curve) is contributed by the 3*d* to 5*p* transition (M_4 edge) of Ru. It may be difficult to decide the peak is generated by carbon or Ru simply by the peak position. However, we can still tell whether C is formed through the intensity of the peak at around 285 eV. When comparing pristine Ru/SS and C@Ru (blue curve), the intensity of the peak is clearly enhanced when carbon presents. Thus, it would be clear when focusing on the 1*s* to π* transition around 285 eV.

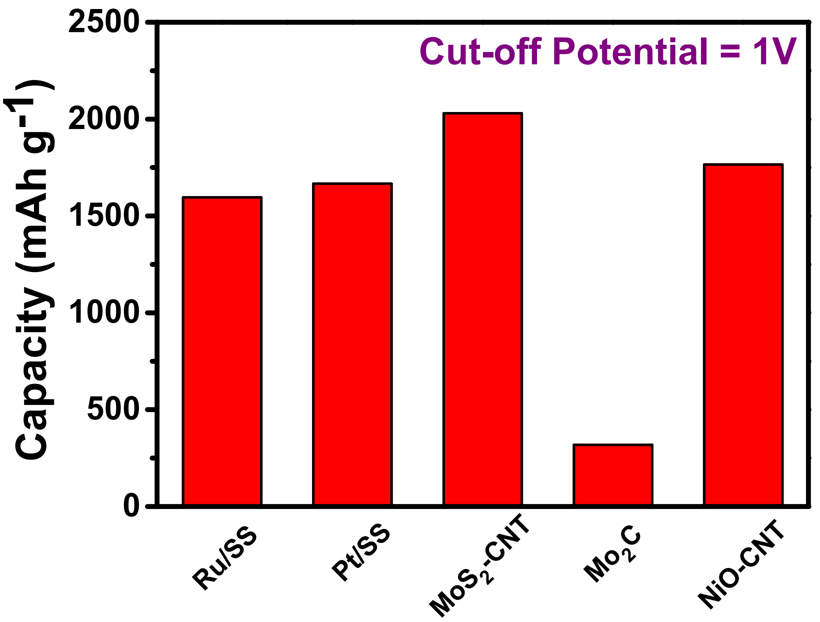

Fig. S9 Full-discharge capacities of Li–CO_2 batteries with five different cathodes. For Pt/SS and Ru/SS, the current density is 15 mA g^{-1} to obtain considerable capacity. The rest of the galvanostatic full-discharge tests are all performed with a current density of 100 mA g^{-1} and a cutoff potential of 1 V.

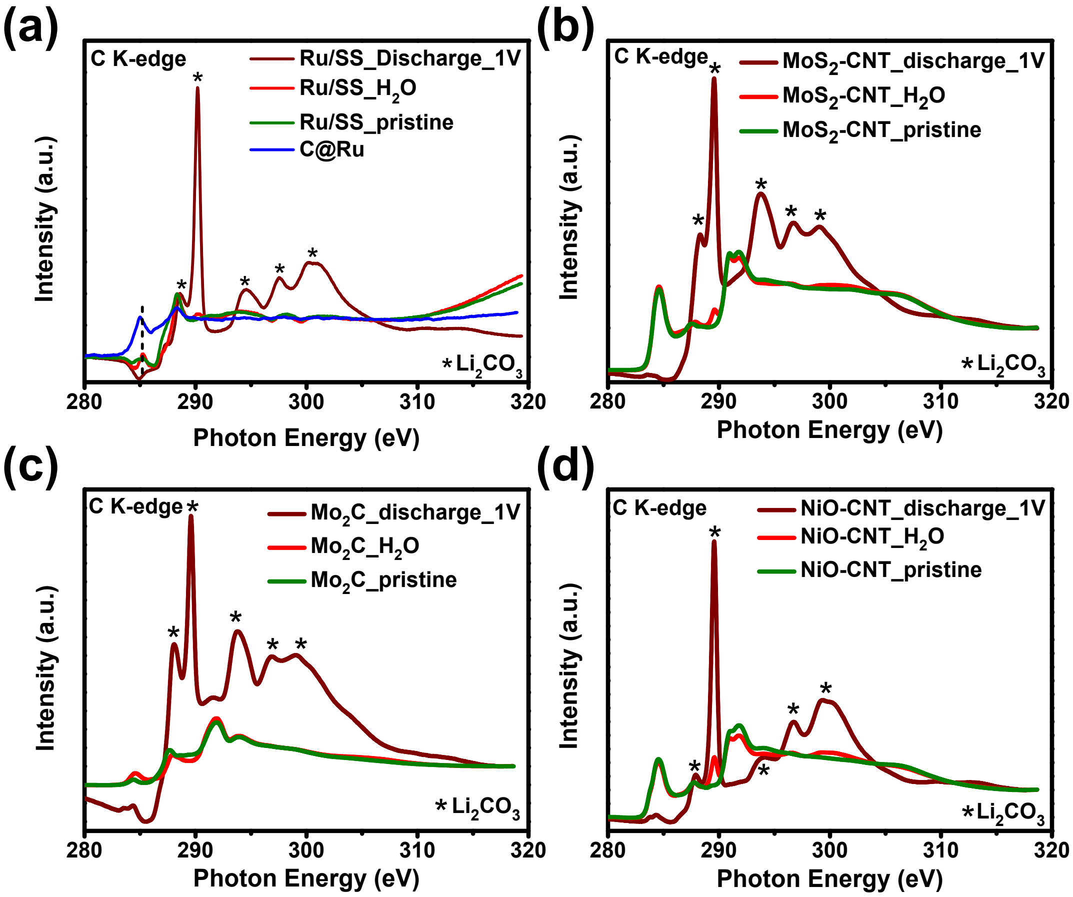

Fig. S10 Soft X-ray absorption spectra of (a) Ru/SS, (b) MoS_2-CNT, (c) Mo_2C, and (d) NiO-CNT under different treatments

The overall trend of SXAS profiles of Ru/SS resembles that of Pt/SS. However, there is a small peak located at around 285 eV for that of pristine Ru/SS. This peak can be attributed to the transition of 3*d* to 5*p* transition (M_4 edge) of Ru. It may be hard to distinguish whether the peak at 285 eV is contributed by carbon or Ru through the peak position. Nevertheless, we can still tell the formation of carbon through the peak intensity. By comparing the SXAS profiles of pristine Ru/SS and C@Ru can we observe a clear peak by carbon. Carbon is thus not observed in the discharged Ru/SS cathodes. The rest of the spectra show high similarity to one of the other. High-intensity peaks of Li_2CO_3 can be observed in all discharged cathodes, while no significant peak is contributed by newly formed carbon. Washing away the formed Li_2CO_3, the profiles of washed cathodes resemble the pristine ones, which again show the absence of carbon.

Fig. S11 Specially designed bottle for electrochemical tests of Li–gas batteries.

Li–gas batteries could be placed in the battery holder inside the bottle. When filling the gas into the glass bottle, the long hollow tube served as an inlet of the gas. A pinhole on the shorter tube was drilled near the bottle cap that enabled the gas inside the bottle to be purged out. After filling the bottle with the desired gas, wires could be connected to the tubes for further electrochemical tests.

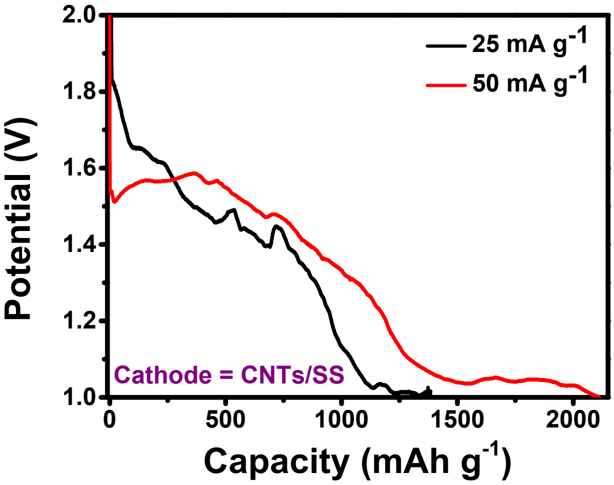

Fig. S12 Galvanostatic full-discharge tests of Li–CO_2 batteries with different current densities. CNTs/SS were used as cathodes in both batteries.

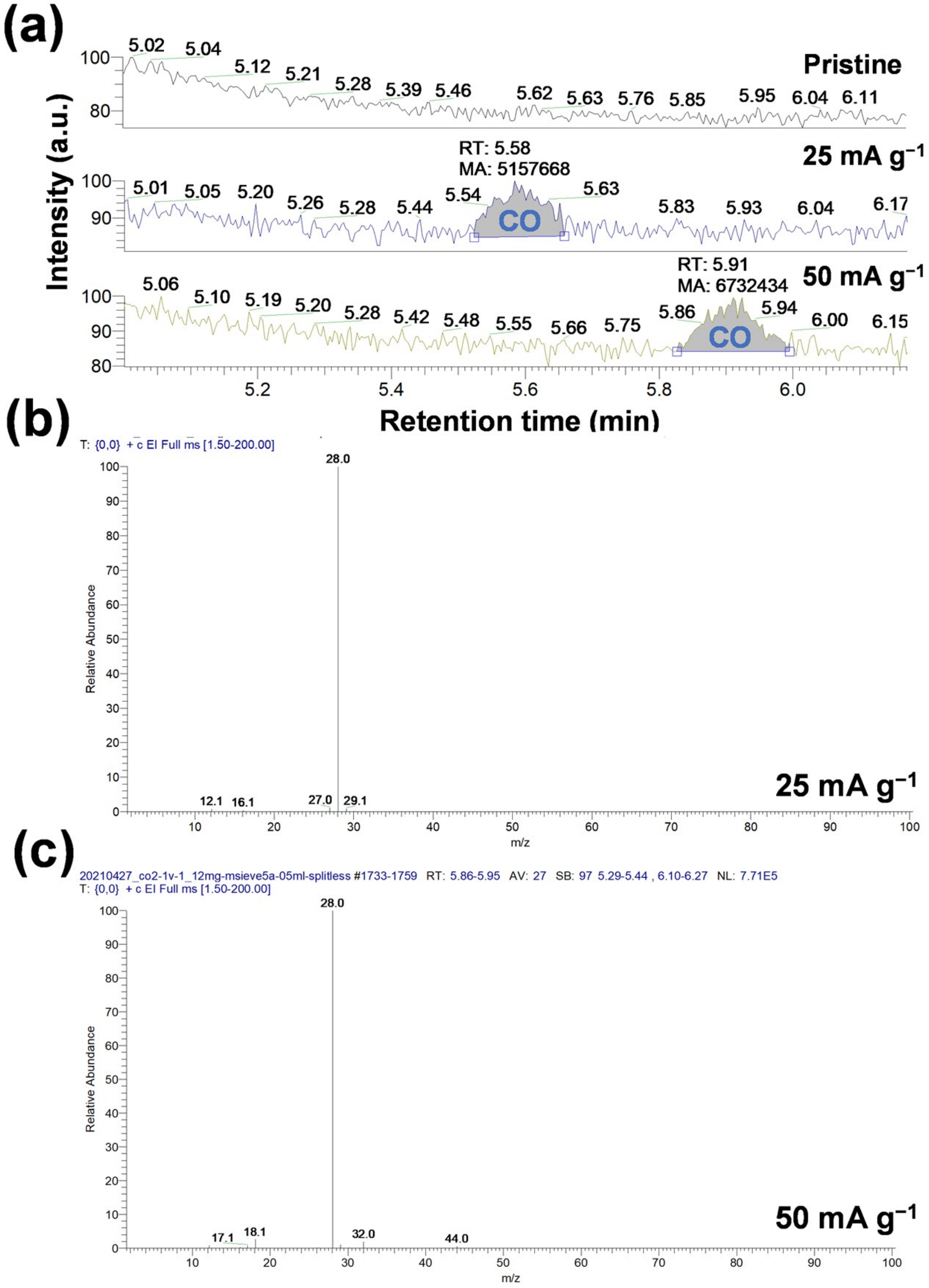

Fig. S13 (a) Gas chromatograms (GC) of the atmosphere of pristine test bottle and discharged Li–CO_2 batteries under different current densities. MS spectra of the detected peaks in (a) for current densities of (b) 25 and (c) 50 mA g^{-1}.

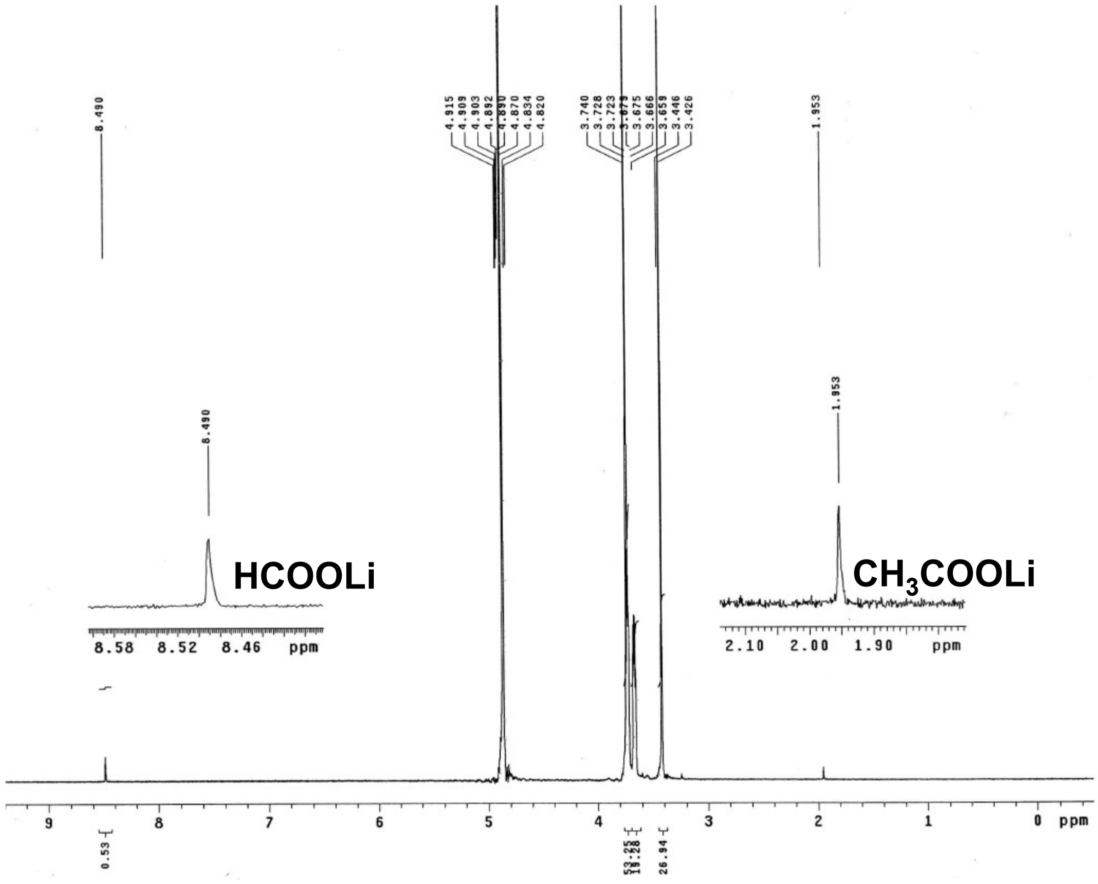

Fig. S14 Nuclear magnetic resonance (NMR) spectra of the electrolyte discharged to 1 V in Li–CO_2 battery, where the peaks of side products (HCOOLi and CH_3COOLi) can be clearly observed.

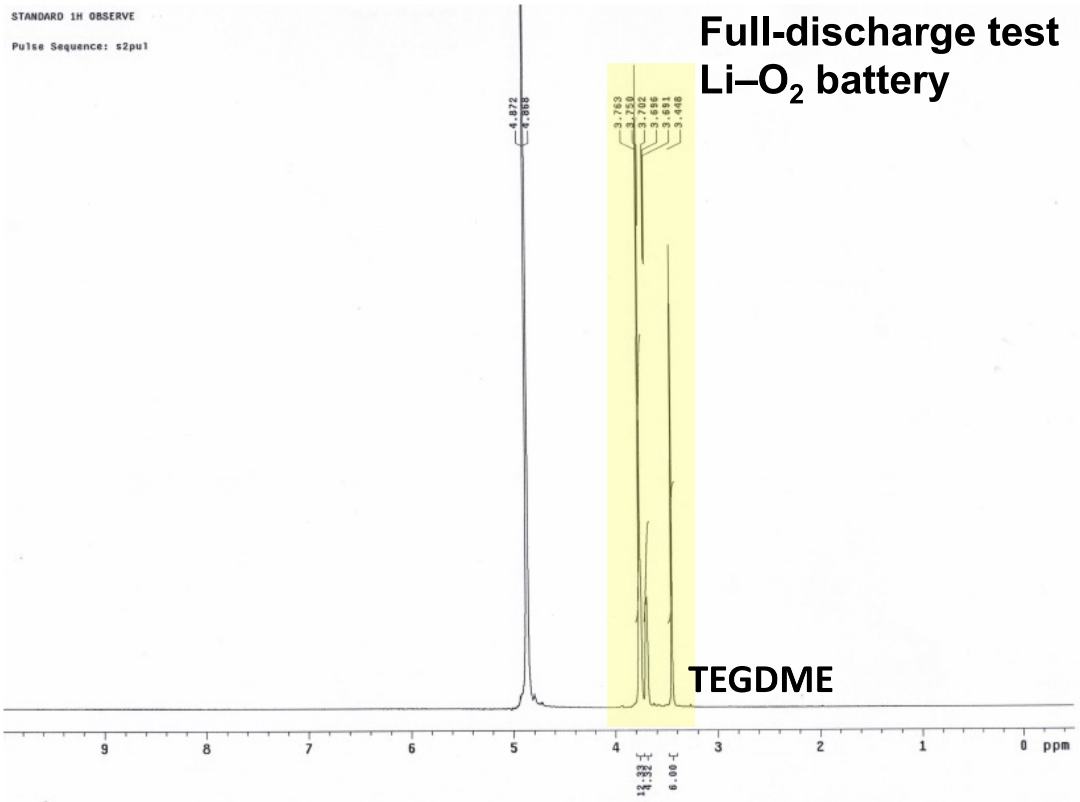

Fig. S15 Nuclear magnetic resonance (NMR) spectrum of the electrolyte discharged to 2 V in Li–O_2 battery. No side products (i.e. HCOOLi and CH_3COOLi) are observed in the spectrum.[3]

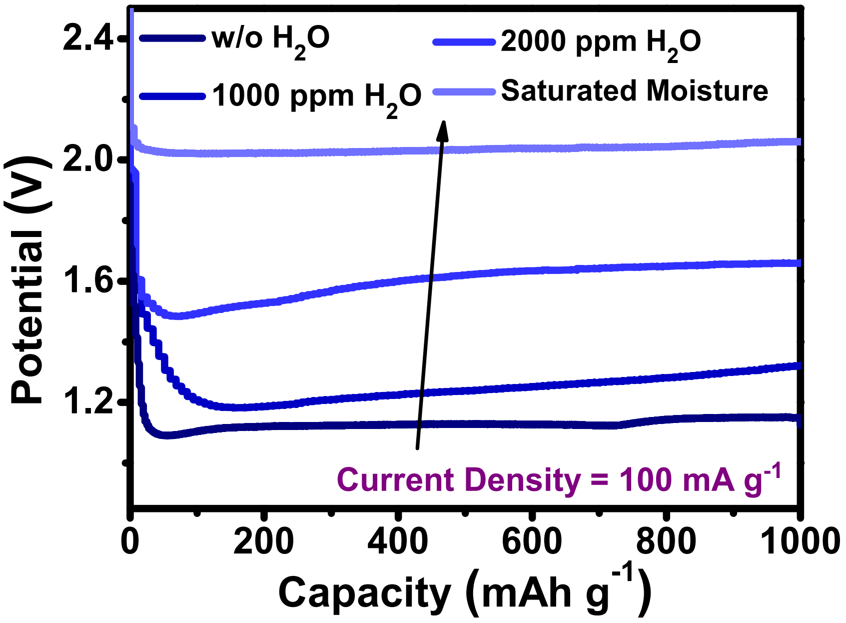

Fig. S16 Galvanostatic discharge tests of Li–CO_2 batteries using CNTs/SS under different contents of water.

Electrolytes with 1000 and 2000 ppm H_2O were used in the discharge tests of Li–CO_2 batteries. Saturated moisture was obtained by adding excess H_2O into the testing bottle.

References

1. S. Thoka, C. M. Tsai, Z. Tong, A. Jena, F.-M. Wang, C. C. Hsu, H. Chang, S. F. Hu and R. S. Liu, *ACS Appl. Mater. Interfaces*, 2020, **13**, 480–490.
2. S. Yang, Y. Qiao, P. He, Y. Liu, Z. Cheng, J.-j. Zhu and H. Zhou, *Energy Environ. Sci.*, 2017, **10**, 972–978.
3. H. Kim, W.-J. Kwak, H.-G. Jung and Y.-K. Sun, *J. Mater. Chem. A*, 2020, **8**, 5622–5628.